

1
2
3
4
5
6
7
8
9
10
11
12
13
14
15
16
17
18
19
20
21
22
23
24
25

Female reproductive fluid composition differs based on mating system in *Peromyscus* mice

Kristin A. Hook¹, Catherine Liu¹, Katherine A. Joyner², Gregg A. Duncan^{2,3}, Heidi S. Fisher^{1*}

1. Department of *Biology*, University of Maryland

1200 *Biology-Psychology Building*

4094 *Campus Drive*

College Park, MD 20742, U.S.A.

2. *Fischell Department of Bioengineering*, University of Maryland

4116 *A. James Clark Hall*

College Park, MD 20742, U.S.A.

3. *Biophysics Program*

University of Maryland

College Park, MD 20742, U.S.A.

*Corresponding author: hfisher@umd.edu

Keywords: cryptic female choice, female control, female reproductive tract, oviduct, post-copulatory sexual selection, reproductive fluid

26 **ABSTRACT**

27

28 Post-copulatory sexual selection is theorized to favor female traits that allow them to control sperm
29 use and fertilization, leading to the prediction that female reproductive traits that influence sperm
30 migration should differ between polyandrous and monogamous species. Here we exploit natural variation
31 in the female mating strategies of closely related *Peromyscus* mice to compare female traits that influence
32 sperm motility – the viscosity, pH, and calcium concentration of fluids in the reproductive tract – between
33 polyandrous and monogamous species. We find that the viscosity and pH, but not calcium concentration,
34 of fluids collected from both the uterus and the oviduct significantly differ between species based on
35 mating system. Our results demonstrate the existence of a viscosity gradient within the female
36 reproductive tract that increases in monogamous species but decreases in polyandrous species. Both
37 species have a more alkaline environment in the uterus than oviduct, but only in the polyandrous species
38 did we observe a decrease in calcium in the distal end of the tract. These results suggest that fluid
39 viscosity and pH in the female reproductive tracts of these mice may be influenced by post-copulatory
40 sexual selection and provide a promising potential mechanism for female sperm control given their
41 importance in modulating sperm behavior.

42

43

44

45

46

47

48

49

50

51 INTRODUCTION

52

53 When females mate with more than one male within a single reproductive cycle (i.e., polyandry),
54 post-copulatory sexual selection is hypothesized to favor male reproductive traits that allow them to
55 outcompete rivals in their race to fertilize a females' ova (i.e., sperm competition; Parker 1970) and
56 female traits that allow them to preferentially bias sperm use in favor of certain males over others (i.e.,
57 cryptic female choice; Thornhill 1983; Eberhard 1996) and to prevent polyspermy (Kim et al. 1996;
58 Firman and Simmons 2013; Firman 2018). Consequently, female reproductive traits that enable post-
59 copulatory control and selective fertilization of ova are predicted to occur in polyandrous – but not
60 monogamous – species. This prediction has been poorly tested, however, likely due to lack of attention to
61 female reproductive traits compared to male reproductive traits in post-copulatory sexual selection studies
62 (Orr et al. 2020), the technical challenges of examining covert mechanisms of 'cryptic female choice' for
63 internally fertilizing species (reviewed in Firman et al. 2017; Ng et al. 2018), and the difficulty of
64 disentangling these female mechanisms from sperm competition and sexual conflict (Simmons and
65 Wedell 2020).

66 Despite the challenges with demonstrating cryptic female choice, several studies across diverse taxa
67 have provided empirical support that females are capable of preferentially biasing and controlling sperm
68 use (reviewed in Firman et al. 2017; Firman 2020). For example, in feral fowl (*Gallus domesticus*),
69 females use muscular contractions to eject sperm from socially subdominant males to prevent
70 insemination and fertilization of their ova (Pizzari and Birkhead 2000); in Japanese macaques (*Macaca*
71 *fuscata*), females increase orgasm-like muscular contractions after mating with a socially dominant male
72 (Troisi and Carosi 1998), which increases sperm retention within their reproductive tract (Baker and
73 Bellis 1993); and in red flour beetles (*Tribolium castaneum*), females appear to be in control of the
74 observed sperm precedence patterns based on male copulatory behavior (Edvardsson and Göran 2000).
75 There is also evidence that physical structures within the female reproductive tract enables female control

76 of sperm use across taxa. For instance, in fruit flies (*Drosophila melanogaster*), female sperm storage
77 organs allow them to control the timing and use of sperm stored after copulation with multiple males
78 (Manier et al. 2010). Moreover, many female vertebrates possess a tube-like passageway to their ovaries
79 (i.e., the oviduct), and there is evidence in birds and mammals that features of this structure (Holt and
80 Fazeli 2016), such as its length (Gomendio and Roldan 1993; Anderson et al. 2006), positively correlate
81 with relative testis size, a proxy for sperm competition level (reviewed in Simmons and Fitzpatrick 2012;
82 Vahed and Parker 2012; Lüpold et al. 2020). These findings suggest that the variable structural
83 architecture of the female reproductive tract may have evolved to regulate sperm uptake (Suarez 2008;
84 Tung and Suarez 2021) by selecting for only those sperm cells that are able to bypass its challenging
85 features (Holt and Fazeli 2016; Suarez 2016) while excluding pathogens or microbes (Tung et al. 2015;
86 Holt and Fazeli 2016; Rowe et al. 2020).

87 The composition of fluids within the female reproductive tract may provide yet another potential
88 mechanism of female control within internally fertilizing species, given that their biochemical properties
89 have been shown to change after insemination, vary throughout the tract, and modulate sperm motility
90 and migration to the ova and, thus, the outcomes of fertilization (reviewed in Holm and Ridderstråle
91 1998; Hunter et al. 2011; Kirkman-Brown and Smith 2011; Holt and Fazeli 2016; Ng et al. 2018;
92 Gasparini et al. 2020). For example, fluids within the reproductive tract can vary in their viscoelastic
93 properties (Johansson et al. 2000; Rodríguez-Martínez et al. 2005; Suarez 2016), which can influence
94 sperm motility patterns and trajectory (Tung et al. 2015; Holt and Fazeli 2016; Tung and Suarez 2021). In
95 humans, mucus coats the entire female reproductive tract, and sperm must swim through viscoelastic
96 cervical mucous as well as the cumulus mass en route to the oocyte (Kirkman-Brown and Smith 2011); a
97 previous study used artificial insemination to demonstrate that this change in fluidic properties effectively
98 serves as a barrier, allowing only more motile and morphologically normal sperm to pass through to the
99 oviduct (Hanson and Overstreet 1981). Moreover, a pH gradient has been demonstrated throughout the
100 female reproductive tract of different mammals, with the uterine environment being more acidic (i.e., less
101 alkaline) than the oviductal environment (reviewed in Ng et al. 2018). Alkaline environments have been

102 shown to increase sperm velocity and induce sperm hyperactivation in mammals, in part through the
103 activation of essential sperm-specific CatSper protein channels (Kirichok et al. 2006; Lishko et al. 2010)
104 that increases sperm intracellular calcium concentrations (Ho and Suarez 2001; Suarez 2008) and
105 subsequently increases their flagella beat frequency and velocity (Brokaw et al. 1974; Suarez et al. 1993).
106 In boars (*Sus scrofa*), high calcium environments lead to greater sperm motility, whereas low calcium
107 environments cause sperm cells to stick to oviductal epithelium and be less motile (Petrunkina et al.
108 2001). Together these studies suggest that the chemical composition of female reproductive fluids
109 provides a promising mechanism for female sperm control driven by post-copulatory sexual selection, but
110 whether these fluidic properties differ between polyandrous and monogamous species remains unknown.

111 In this study, we test whether the composition of female reproductive tract fluids diverge between
112 species that have evolved under divergent mating systems in *Peromyscus* mice. More specifically, we
113 collected fluids from two distinct regions of the reproductive tract – the uterus and the oviduct – for three
114 polyandrous species (*P. maniculatus*, *P. leucopus*, and *P. gossypinus*) and their closely related
115 monogamous congeners (*P. californicus*, *P. eremicus*, and *P. polionotus*; Turner et al. 2010; Bedford and
116 Hoekstra 2015). From these fluids, we measured viscosity, pH, and calcium concentration, all of which
117 have been shown to significantly impact sperm movements in other taxa. We compared these
118 physiological properties between species that evolved under polyandry to those that evolved under
119 monogamy to examine associations between mating strategy and potential mechanisms of post-copulatory
120 female control. From these data, we were also able to establish for each species whether a gradient for
121 each of these properties exists within the reproductive tract and indirectly assess how that might impact
122 sperm motility and their unique ability to form collective groups within these mice (Hook et al. 2022).

123

124 **MATERIALS AND METHODS**

125

126 **Female fluid collection**

127 We obtained captive *Peromyscus maniculatus bairdii*, *P. polionotus subgriseus*, *P. leucopus*, *P.*
128 *eremicus*, and *P. californicus insignis* from the Peromyscus Genetic Stock Center at the University of
129 South Carolina, and *P. gossypinus* from Dr. Hopi Hoekstra at Harvard University. We housed the mice in
130 same-sex cages at 22°C on a 16L:8D cycle in accordance with guidelines established by the Institutional
131 Animal Care and Use Committee at the University of Maryland (protocol # R-Jul-18-38). We sought
132 samples from all available captive *Peromyscus* species and avoided wild-caught specimens to control for
133 variation due to age, nutrition, and sexual experience. We collected fluid from females in estrus
134 (identified by methods in Byers et al., 2012) to reduce variation associated with the estrous cycle (Hunter
135 et al. 2011; Simons and Olson 2018). We euthanized all focal females via isoflurane overdose and
136 cervical dislocation prior to removing the reproductive tract for fluid extraction.

137

138 **Collecting fluid and particle tracking microrheology (PTM)**

139 To collect fluid for viscosity measurements, we removed the female reproductive tract and submersed
140 it in mineral oil at 4°C until fluid extraction, which took place within 24 hours. To visually distinguish the
141 mineral oil from biological fluid, we dyed the oil blue using a colored gel dye (Wilton Candy Colors,
142 USA) in a 1:75 dye:oil ratio. Under 0.63x magnification (Zeiss Stemi 508, USA), we trimmed the fat
143 surrounding the reproductive tract, unraveled the coiled oviducts, severed the uterus from the oviduct at
144 the utero-tubal junction (UTJ), divided the oviduct in half to separate the lower and upper regions, and
145 submersed in dyed mineral oil. We used glass Pasteur pipettes bent into a u-shape under a flame to push
146 down from one end of the tissue to the other to squeeze fluid within the tissue out into the oil, then
147 collected and centrifuged the samples, removed the oil supernatant and stored fluids at -80°C (Yuana et al.
148 2015; Patczai et al. 2017).

149 To obtain sufficient volume for downstream methods, we pooled the samples for each region from at
150 least ten individuals per species, then warmed pools to 37°C to simulate natural physiological values, and
151 again centrifuged at 3000 rpm for 3 min to ensure full separation of the mineral oil from the reproductive
152 fluid. We then combined 2µL of fluid with 0.5µL of ~0.002% w/v suspension of fluorescent nanoparticles

153 (PEG-coated polystyrene particles, PS-PEG). PS-PEG were prepared by coating red fluorescent
154 carboxylate-modified PS spheres (PS-COOH), 500 nm in diameter (ThermoFisher FluoSpheres
155 Carboxylate-Modified Microspheres, 0.5 μm , red fluorescent (580ex/605em), 2% solids, USA) with 5-
156 kDa methoxy-PEG-amine (Creative PEG-Works, USA) via NHS-ester chemistry as previously described
157 (Joyner et al. 2019). We gently reverse-pipetted the mixture to make sure the nanoparticles were
158 homogeneously scattered throughout and pipetted 2.0 μL into a 1-mm ID Viton O-ring microscopy
159 chamber (McMaster Carr, USA) and covered with a small circular glass coverslip, both of which were
160 sealed with vacuum grease (Dow Corning, USA) to prevent fluid flow and evaporation, and equilibrated
161 for 30 minutes prior to imaging to reduce dynamic error.

162 To measure viscosity, we recorded a minimum of three videos of the suspended fluorescent
163 nanoparticles within each fluid sample at a frame rate of 33.33 Hz for 300 frames (10 sec) using an
164 EMCCD camera (Axiocam 702; Zeiss, Germany) attached to an Zeiss 800 LSM inverted microscope and
165 x63/1.20 W Korr UV VIS IR water-immersion objective with image resolution of 0.093 μm per pixel. To
166 avoid edge effects on nanoparticle movement, we randomly selected central locations within the chamber
167 for our video recordings. All samples remained at 37°C during imaging using a stage incubator (PM 2000
168 Rapid Balanced Temperature, PeCon, Germany). To track the diffusion of PS-PEG nanoparticles in each
169 sample, we used particle tracking data analysis using automated software custom-written in MATLAB
170 (Mathworks, USA). Based on a previously developed algorithm (Crocker and Grier 1996), the program
171 determined the x and y positions of nanoparticle centers based on an intensity threshold and then
172 constructed particle trajectories by connecting particle centers between sequential images given an input
173 maximum moving distance between frames. Finally, the program calculated the time-averaged mean
174 squared displacement [MSD (τ)] as

$$175 \quad \langle \Delta r^2(\tau) \rangle = \langle [x(t+\tau) - x(t)]^2 + [y(t+\tau) - y(t)]^2 \rangle$$

176 where τ is the time lag between frames and angle brackets denote the average over the time points. The
177 MSD of PS-PEG nanoparticles is directly proportional the viscosity of the surrounding fluid. A fast-

178 moving particle (high MSD) reflects a low viscosity fluid whereas a slow-moving particle (low MSD)
179 reflects a high viscosity fluid. Using the generalized Stokes–Einstein relation, measured MSD values were
180 used to compute viscoelastic properties of the hydrogels (Joyner et al. 2020). The Laplace transform of $\langle \Delta r^2(\tau) \rangle$, $\langle \Delta r^2(s) \rangle$, is related to viscoelastic spectrum $G(s)$ using the equation $G(s) = 2k_B T / [\pi a s \langle \Delta r^2(s) \rangle]$,
181 where $k_B T$ is the thermal energy, a is the particle radius, s is the complex Laplace frequency. The complex
182 modulus can be calculated as $G^*(\omega) = G'(\omega) + G''(i\omega)$, with $i\omega$ being substituted for s , where i is a
183 complex number and ω is frequency. We pooled these data across all particles to characterize female
184 reproductive fluid viscosity per species. Due to technical difficulties, we were unable to collect viscosity
185 data from the upper oviduct for two of the polyandrous species (*P. maniculatus* and *P. gossypinus*). For
186 this reason, we combined viscosity data for both the lower and upper oviducts into a single measure for
187 every focal species.

189

190 **Collecting and measuring fluid pH and calcium**

191 Due to the limited quantity of fluids collected from each female reproductive tract for our viscosity
192 measurements, we were not able to also measure pH and calcium using these same individuals. Because
193 we were further limited by the number of available animals in our lab colony, we focused on two species
194 in which ten females were available for this study – the polyandrous *P. maniculatus* and its monogamous
195 sister-species *P. polionotus*. To extract reproductive fluid for these measurements, we dissected the
196 reproductive tract, reserved the right side of each tract for the pH measurements and submersed the left
197 side of each tract into phosphate buffer solution (PBS) at 4°C for the calcium measurements.

198 To measure the pH of reproductive fluids, we placed pH strips (Hydrion [9400] Spectral 5.0-9.0) on
199 microscope slides (VWR Plastic Microslides, USA) on a 37°C warmer (Fisherbrand Isotemp Digital Dry
200 Bath/Block Heater, USA) and under 0.63X magnification (Zeiss Stemi 2000, USA). We trimmed the fat,
201 unraveled the coiled oviduct, placed the elongated tract on a pH strip, and severed the uterus from the
202 oviduct at the UTJ. We then placed the oviduct on another pH strip, cut it in half, pinched the open end of

203 the lower oviduct closed with forceps, and placed it on a third pH strip. We used separate u-shaped glass
204 pipettes to push from one end of each region of the reproductive tract to the other end to squeeze fluid out
205 onto the pH strip to measure pH immediately after release from the tissue (Yeung et al. 2004).

206 To measure calcium in reproductive fluids, we used a calcium assay kit (Abcam Calcium Assay Kit
207 ab102505, USA). After removing the tissue from PBS, we severed the uterus from the oviduct at the UTJ,
208 cut the oviduct in half to separate the lower and upper oviducts, placed each tissue region in a separate
209 tube containing calcium assay buffer, and ground the tissues with disposable plastic pestles
210 (ThermoFisher, USA). We separated the tissue from the buffer and reproductive fluid by centrifuging at
211 4°C for 5 min at 3500 rpm (Eppendorf Centrifuge 5702RH, USA), pipetted the supernatant from each
212 tract region into microplate wells (CellStar 96 Well Cell Culture Plate, USA), added the chromogenic
213 reagent, calcium assay buffer, and calcium standard, and immediately measured the mixture's absorbance
214 at 575nm using a microplate reader (Thermo Scientific Multiskan FC, USA).

215

216 **Statistical analyses**

217 We performed all statistical analyses using R version 3.4.2 (R Core Team 2016) and created all
218 figures using the 'ggplot2' package with R (Wickham 2016). We visually inspected all diagnostic plots
219 (qqplots and plots of the distribution of the residuals against fitted values) to validate model normality. In
220 cases where model assumptions of normality were not, we assessed the normality of the response variable
221 using a Shapiro-Wilk test and transformed variables as needed until normality of models was met. Only
222 the best fitting models are reported here.

223 To assess differences in the viscosity of female reproductive fluids between polyandrous and
224 monogamous species, we used our dataset of individually tracked particles and pooled these data across
225 species with shared mating systems (categorized as either monogamous or polyandrous). We excluded
226 data that were $\pm 2SD$ of the mean within each sample because they represented clear outliers. All viscosity
227 values were log-transformed to improve model assumptions of normality. We assessed differences in the
228 viscosity of female reproductive fluids in the uterus and in the oviduct using separate linear models (LM),

229 with log viscosity as the response variable and mating system as the predictor variable. We also analyzed
230 fluidic differences in each tract region within each species using separate linear models, with log viscosity
231 as the response variable and the region of the female reproductive tract as the predictor variable. Last, we
232 used the data sets from three focal samples (*P. eremicus*, *P. gossypinus*, and *P. polionotus*) to statistically
233 compare viscosity measurements to their dyed mineral oil controls using separate linear models, with log
234 viscosity as the response variable and the sample type as the predictor variable. Post-hoc pairwise
235 comparisons were made using Tukey HSD adjustments for multiple comparisons using the ‘LSmeans’ R
236 package (Lenth 2016).

237 To assess differences in the pH and calcium levels of female reproductive fluids between polyandrous
238 and monogamous species, we used separate linear models for each region of the tract, with either pH or
239 the log calcium measurements included as the response variable and mating system included as the
240 explanatory variable. Last, we used paired t-tests to conduct pairwise comparisons for pH and calcium
241 measurements from each region of the tract within each species to control for differences among
242 individual females.

243

244 **RESULTS**

245

246 All fluid viscosity measures collected from the female reproductive tracts of each focal *Peromyscus*
247 species are reported in Table 1. We found that the viscosity of fluids in both the uterus and the oviduct
248 significantly differed based on mating system in *Peromyscus* mice. More specifically, polyandrous
249 species have significantly more viscous fluid in the uterus (LM: $F_{1,1255} = 27.09$, $p < 0.001$) but
250 significantly less viscous fluid in the oviduct (LM: $F_{1,1755} = 24.7$, $p < 0.001$) than monogamous species
251 (Figure 1). Within-species analyses revealed that fluids were significantly more viscous when collected
252 from the uterus compared to the oviduct in *P. maniculatus*, *P. leucopus*, and *P. californicus*, but the
253 opposite was true in *P. eremicus* and *P. polionotus*; no difference was observed in the viscosity of uterine
254 fluid or oviductal fluid in *P. gossypinus*, however (Table 1).

255 We found that the reproductive fluid pH of the focal polyandrous species, *P. maniculatus*, was
256 significantly higher within the uterus (LM: $F_{1,18} = 17.05$ $p < 0.001$) and oviduct (LM: $F_{1,18} = 14.39$, $p <$
257 0.01) compared to its monogamous congener, *P. polionotus* (Table 2, Figure 2). However, we found no
258 differences in calcium concentrations between these species in either the fluids collected from the uterus
259 (LM: $F_{1,18} = 2.005$, $p = 0.174$) or from the oviduct (LM: $F_{1,18} = 0.3423$, $p = 0.566$; Table 2, Figure 3).
260 Within both species, the fluid collected from the uterus had a significantly higher pH than the oviduct
261 (paired t-test: *P. maniculatus* $t = 21$, $df = 9$, $p < 0.001$; *P. polionotus* $t = 6.986$, $df = 9$, $p < 0.001$; Figure
262 2). In *P. maniculatus*, the fluid collected from the uterus was significantly more calcemic (paired t-test: t
263 $= 3.95$, $df = 9$, $p < 0.01$), a pattern that was not observed in *P. polionotus* (paired t-test: $t = 1.98$, $df = 9$, p
264 $= 0.079$).

265

266 **DISCUSSION**

267

268 Reproductive traits are among the most rapidly evolving traits in nature and are driven by many
269 evolutionary processes, including post-copulatory sexual selection (e.g., Eberhard 2004; Clark et al. 2006;
270 Martin-Coello et al. 2009; Ramm et al. 2009). In polyandrous systems, sperm from multiple partners are
271 expected to interact and compete for fertilization of the available ova, and females are predicted to evolve
272 traits that allow them to exert control over the outcome of this competition (reviewed in Eberhard 1996;
273 Firman et al. 2017). In this study, we asked whether female reproductive traits that impact the successful
274 migration of sperm to the site of fertilization differ between polyandrous and monogamous species. We
275 examined the composition of fluids collected from the two reproductive organs closest to the fertilization
276 site – the oviduct and the uterus – using *Peromyscus* mice with naturally variable mating systems among
277 closely related species. Our results show that (1) polyandrous species have significantly more viscous
278 fluid in the uterus but less viscous fluid in the oviduct than monogamous species, and a viscosity gradient
279 from the uterus to the oviduct increases in monogamous species but decreases in polyandrous species; (2)

280 the reproductive fluid pH is significantly higher in the uterus and oviduct of the polyandrous *P.*
281 *maniculatus* compared to its monogamous congener, *P. polionotus*, but both species have a more alkaline
282 environment in the uterus than oviduct overall; and (3) there are no differences in the calcium content
283 between species, but *P. maniculatus* has a calcium gradient that decreases at the distal end of the
284 reproductive tract. Given that these traits and their interactions are likely to affect sperm motility and
285 migration toward the site of fertilization, these fluidic properties warrant further study to determine the
286 extent to which they provide females control of sperm use within these mice.

287 Using a highly sensitive method (Duncan et al. 2016), we found that polyandrous species (*P.*
288 *maniculatus*, *P. leucopus*, and *P. gossypinus*) have significantly more viscous fluid in the uterus but less
289 viscous fluid in the oviduct than their closely related monogamous congeners (*P. californicus*, *P.*
290 *eremicus*, and *P. polionotus*). *In vitro* experiments in *Peromyscus* have shown that increasing the
291 viscosity of the microenvironment leads to reduced sperm velocity (Hook et al. 2022), consistent with
292 other systems (Smith et al. 2009; Miki and Clapham 2013). Our findings suggest that in polyandrous
293 species, sperm motility is hindered more in the uterus, which is closest to the sperm entry site and
294 therefore provides an initially more competitive environment that likely selects for the most motile sperm
295 prior to ever reaching the oviduct (Holt and Fazeli 2016; Suarez 2016). The opposite pattern was
296 observed in the monogamous species, in which sperm motility would be enhanced in the uterus but
297 hindered in the oviduct. In these monogamous species, it is possible that the UTJ – a constricted
298 passageway that separates these two tract regions and contains highly viscous fluid in other species
299 (reviewed in Hunter 1995) – provides an adequately effective barrier to remove morphologically
300 abnormal and slower sperm (Chatdarong et al. 2004; Druart 2012), as has been observed in a previous
301 study examining their collective sperm groups (Hook et al. 2022), and that the higher oviductal fluid
302 viscosity is effective in reducing sperm motility and, thus, the possibility of polyspermy (Kim et al. 1996;
303 Firman and Simmons 2013; Firman 2018). Overall, the significant differences in fluid viscosity based on
304 mating systems is suggestive of an association with post-copulatory sexual selection. Further studies are
305 warranted in these species to examine how sperm interact with uterine and oviductal fluids, as well as

306 seminal fluids after mating (Miki and Clapham 2013), to transverse the UTJ and reach the fertilization
307 site given these observed differences in female fluidic viscosity.

308 We also found that the reproductive fluid pH is significantly higher in the uterus and oviduct of the
309 polyandrous deer mouse (*P. maniculatus*) during estrus compared to its monogamous congener, *P.*
310 *polionotus*, but that both species have a more alkaline environment in the uterus than oviduct. This result
311 is surprising given that the opposite has been observed in other studies (López-Albors et al. 2021, but see
312 Ng et al. 2018). Such alkaline environments have been shown to enhance sperm motility in birds (*Gallus*
313 *domesticus*, *Coturnix coturnix*, *Meleagris gallopavo*; Holm and Wishart 1998) and humans (Saito et al.
314 1996; Zhou et al. 2015), and to activate sperm-specific CatSper channels in mice (*Mus musculus*;
315 Kirichok et al. 2006) and humans (Lishko et al. 2010), thereby inducing sperm hyperactivation (Suarez et
316 al. 1993). Sperm hyperactivation, which takes place in the lower oviduct in rabbits (Overstreet and
317 Cooper 1979) and mice (Suárez and Osman 1987), is an important sperm movement pattern characterized
318 by a deep flagellar bend (reviewed in Suarez and Ho 2003). In bulls, sperm cells exhibit deep
319 asymmetrical bends in pH 7.9-8.5 solutions and shallow asymmetrical bends in pH 7.0-7.5 solutions (Ho
320 et al. 2002). We found that the average pH in upper oviduct fluid was 7.44 in *P. maniculatus* and 7.28 in
321 *P. polionotus*, which is consistent with shallow asymmetrical bends in hyperactivated sperm in both
322 species. Our finding that this trait differs between species based on mating system suggests it might be a
323 trait that is driven by post-copulatory sexual selection, although the greater pH of fluids in the
324 polyandrous species suggests this trait is enabling them to have greater sperm motility, rather than
325 hindering their movement or serving as a barrier for movement. Further studies are warranted to verify
326 the effects of pH on *Peromyscus* sperm movements *in vivo* and how this trait synergistically interacts with
327 the viscosity or calcemic contents of female reproductive fluids or impacts the ability of sperm to
328 capacitate (Stival et al. 2016) or form collective groups that swim together (Fisher and Hoekstra 2010;
329 Hook et al. 2022).

330 Last, we found that the concentration of calcium in the uterine and oviductal fluids extracted from the
331 polyandrous *P. maniculatus* and monogamous *P. polionotus* did not significantly differ. If this fluidic

332 component enables female control of sperm use, we would expect a difference between these species that
333 differ by mating system. However, it is interesting to note that only in *P. maniculatus* did we observe a
334 gradient in which calcium concentration decreases moving up the female reproductive tract from the
335 uterus to the oviduct. There is a positive association between extracellular calcium and sperm velocity in
336 humans (Zhou et al. 2015), rats (Lindemann and Goltz 1988), and hamsters (Suarez and Dai 1995), which
337 suggests that the reduction in calcemic contents in the oviductal fluids of the polyandrous *P. maniculatus*
338 may impose a barrier on sperm motility. Alternatively, it may indicate that sperm hyperactivate much
339 earlier in *P. maniculatus*, given that calcium is essential for sperm hyperactivation (Yanagimachi 1982),
340 and increases in extracellular calcium levels increase calcium entry through sperm-specific CatSper
341 channels (Marquez and Suarez 2007). We cannot rule out that this property interacts with other fluidic
342 properties or with seminal fluids to control sperm migration, so future studies that examine these effects –
343 specifically through *in vivo* experiments and accounting for potential interspecies variation in these
344 fluidic properties – are warranted.

345 Our results demonstrate some important differences in the fluid collected from different regions of the
346 female reproductive tract, however finer-scale changes in more localized areas of the reproductive tract
347 and in response to seminal fluids will further enhance our understanding of how selection has shaped the
348 fertilization environment in *Peromyscus*. Our understanding of the physiological mechanisms required for
349 mammalian fertilization remain obscure without the ability to measure conditions *in vivo* in real-time (Ng
350 et al. 2018), especially in small animals, but our results suggest that even closely-related species may
351 exhibit striking differences similar in magnitude to differences in highly divergent taxa (López-Albors et
352 al. 2021). In other mammals, evidence suggests that uterine fluid near the cervix is more viscous than
353 more proximal regions of the uterus, and oviductal fluid in the ampullary region contains viscous
354 compounds produced from ovulating follicles and peritoneal fluid during estrus (reviewed in Hunter et al.
355 2011). In bovine, for example, the greater amount mucus in the ampulla compared to lower regions of the
356 oviduct is associated with reduced sperm numbers near the fertilization site (Suarez et al. 1997). Our
357 study was limited by the small quantity of fluid we could extract from *Peromyscus* oviducts – although

358 we aimed to maximize this with our approach. The comparisons we were able to make between fluid
359 obtained from the isthmus and ampullary regions suggest that fluidic properties in the oviduct may be
360 equally as dynamic as the structural features (e.g., Yániz et al. 2000; Suarez 2016; Miller 2018).

361 Taken together, our results support the prediction that female reproductive fluids can vary by the
362 species' mating system, and thus level of post-copulatory sexual selection, yet the directionality of the
363 differences make their functional significance less clear. We found that female reproductive fluids in
364 polyandrous species is more acidic with differing viscosities throughout the tract compared to
365 monogamous *Peromyscus* females. We also found variation between distinct regions of the reproductive
366 tract, providing indirect evidence for how these properties might impact sperm cells as they migrate up
367 toward the site of fertilization. Our results suggest that fluid viscosity and pH may provide promising
368 avenues for investigating a female reproductive trait that is driven by cryptic female choice, although
369 follow-up experiments are needed to assess their impacts on sperm motility *in vivo* and on male
370 fertilization success within a competitive context.

371

372 **Data Availability Statement:** All data are available in Dryad.

373

374 **Competing Interests:** We declare we have no competing interests.

375

376 **Author Contributions:** KAH, HSF, and CL conceived of the study, designed experiments, and
377 interpreted results; CL, KAH, and KAJ collected the data, KAJ analyzed video data, KAH carried out the
378 statistical analyses; all authors wrote the manuscript and all authors gave final approval for publication.

379

380 **Acknowledgements:** We are grateful to Hopi Hoekstra for providing *P. gossypinus* males and to Erica
381 Gasper for providing *P. californicus* males and providing use of a microplate reader. Thanks to W. David
382 Weber for help in determining estrous phase of female mice, maintaining the mouse colony, and

383 collecting many of the reproductive tracts analyzed for this study. We thank Mollie Manier, Halli Weiner,
384 and Patricia Martin-DeLeon for advice on methods for measuring calcium and pH and Shelby Wilson for
385 statistical advice. Thanks to Harrison Arsis, Madeline-Sophie Dang, Catherine Liu, and Audrey Mvemba
386 for their assistance with video analyses. Funding was provided by a National Science Foundation
387 Postdoctoral Research Fellowship [1711817] to KAH, a University of Maryland Honors College
388 Research Grant to CL, the Cystic Fibrosis Foundation (JOYNER18FO) to KAJ, a Burroughs Wellcome
389 Fund Career Award at the Scientific Interface to GAD, and a Eunice Kennedy Shriver National Institute
390 of Child Health and Human Development K99/R00 Pathway to Independence Award [R00HD071972] to
391 HSF.

392

393 **LITERATURE CITED**

394

- 395 Anderson, M. J., A. S. Dixson, and A. F. Dixson. 2006. Mammalian sperm and oviducts are sexually
396 selected: evidence for co-evolution. *Journal of Zoology* 270:682–686.
- 397 Baker, R. R., and M. A. Bellis. 1993. Human sperm competition: ejaculate manipulation by females and a
398 function for the female orgasm. *Animal Behaviour* 46:887–909.
- 399 Bedford, N. L., and H. E. Hoekstra. 2015. The natural history of model organisms: *Peromyscus* mice as a
400 model for studying natural variation. *eLife* 4:e06813.
- 401 Brokaw, C. J., R. Josslin, and L. Bobrow. 1974. Calcium ion regulation of flagellar beat symmetry in
402 reactivated sea urchin spermatozoa. *Biochemical and Biophysical Research Communications*
403 58:795–800.
- 404 Chatdarong, K., C. Lohachit, and C. Linde-Forsberg. 2004. Distribution of spermatozoa in the female
405 reproductive tract of the domestic cat in relation to ovulation induced by natural mating.
406 *Theriogenology* 62:1027–1041.

- 407 Clark, N. L., J. E. Aagaard, and W. J. Swanson. 2006. Evolution of reproductive proteins from animals
408 and plants. *Reproduction* 131:11–22. Society for Reproduction and Fertility.
- 409 Crocker, J. C., and D. G. Grier. 1996. Methods of Digital Video Microscopy for Colloidal Studies.
410 *Journal of Colloid and Interface Science* 179:298–310.
- 411 Druart, X. 2012. Sperm Interaction with the Female Reproductive Tract. *Reproduction in Domestic*
412 *Animals* 47:348–352.
- 413 Duncan, G. A., J. Jung, A. Joseph, A. L. Thaxton, N. E. West, M. P. Boyle, J. Hanes, and J. S. Suk. 2016.
414 Microstructural alterations of sputum in cystic fibrosis lung disease. *JCI Insight* 1:e88198.
- 415 Eberhard, W. 1996. *Female Control: Sexual Selection by Cryptic Female Choice*. Princeton, NJ:
416 Princeton University Press.
- 417 Eberhard, W. G. 2004. Rapid Divergent evolution of sexual morphology: comparative tests of
418 antagonistic coevolution and traditional female choice. *Evolution* 58:1947–1970.
- 419 Edvardsson, M., and A. Göran. 2000. Copulatory courtship and cryptic female choice in red flour beetles
420 *Tribolium castaneum*. *Proceedings of the Royal Society of London. Series B: Biological Sciences*
421 267:559–563.
- 422 Firman, R. C. 2020. Of mice and women: advances in mammalian sperm competition with a focus on the
423 female perspective. *Philosophical Transactions of the Royal Society B: Biological Sciences*
424 375:20200082.
- 425 Firman, R. C. 2018. Postmating sexual conflict and female control over fertilization during gamete
426 interaction. *Annals of the New York Academy of Sciences* 1422:48–64.
- 427 Firman, R. C., C. Gasparini, M. K. Manier, and T. Pizzari. 2017. Postmating Female Control: 20 Years of
428 Cryptic Female Choice. *Trends in Ecology & Evolution* 32:368–382.
- 429 Firman, R. C., and L. W. Simmons. 2013. Sperm competition risk generates phenotypic plasticity in
430 ovum fertilizability. *Proceedings of the Royal Society B: Biological Sciences* 280:20132097.
- 431 Fisher, H. S., and H. E. Hoekstra. 2010. Competition drives cooperation among closely related sperm of
432 deer mice. *Nature* 463:801.

- 433 Gasparini, C., A. Pilastro, and J. P. Evans. 2020. The role of female reproductive fluid in sperm
434 competition. *Philosophical Transactions of the Royal Society B: Biological Sciences*
435 375:20200077.
- 436 Gomendio, M., and E. R. S. Roldan. 1993. Coevolution between male ejaculates and female reproductive
437 biology in eutherian mammals. *Proceedings of the Royal Society of London. Series B: Biological*
438 *Sciences* 252:7–12.
- 439 Hanson, F. W., and J. W. Overstreet. 1981. The interaction of human spermatozoa with cervical mucus in
440 vivo. *American Journal of Obstetrics and Gynecology* 140:173–178.
- 441 Ho, H. C., K. A. Granish, and S. S. Suarez. 2002. Hyperactivated motility of bull sperm is triggered at the
442 axoneme by Ca²⁺ and not cAMP. *Developmental Biology* 250:208–217.
- 443 Ho, H. C., and S. S. Suarez. 2001. An inositol 1,4,5-trisphosphate receptor-gated intracellular Ca²⁺ store
444 is involved in regulating sperm hyperactivated motility1. *Biology of Reproduction* 65:1606–1615.
- 445 Holm, L., and Y. Ridderstråale. 1998. Localization of carbonic anhydrase in the sperm-storing regions of
446 the turkey and quail oviduct. *The Histochemical Journal* 30:481–488.
- 447 Holm, L., and G. J. Wishart. 1998. The effect of pH on the motility of spermatozoa from chicken, turkey
448 and quail. *Animal Reproduction Science* 54:45–54.
- 449 Holt, W. V., and A. Fazeli. 2016. Sperm selection in the female mammalian reproductive tract. Focus on
450 the oviduct: Hypotheses, mechanisms, and new opportunities. *Theriogenology* 85:105–112.
- 451 Hook, K. A., W. D. Weber, and H. S. Fisher. 2022. Postcopulatory sexual selection is associated with
452 sperm aggregate quality in *Peromyscus* mice. *Behavioral Ecology* 33:55–64.
- 453 Hunter, R. H. F. 1995. How, when, and where do spermatozoa gain their fertilising ability in vivo?
454 *Reproduction in Domestic Animals* 31:51–55.
- 455 Hunter, R. H. F., P. Coy, J. Gadea, and D. Rath. 2011. Considerations of viscosity in the preliminaries to
456 mammalian fertilisation. *Journal of Assisted Reproduction and Genetics* 28:191–197.

- 457 Johansson, M., P. Tienthai, and H. Rodríguez-Martínez. 2000. Histochemistry and ultrastructure of the
458 intraluminal mucus in the sperm reservoir of the pig oviduct. *Journal of Reproduction and*
459 *Development* 46:183–192.
- 460 Joyner, K., D. Song, R. F. Hawkins, R. D. Silcott, and G. A. Duncan. 2019. A rational approach to form
461 disulfide linked mucin hydrogels. *Soft Matter* 15:9632–9639.
- 462 Kim, N.-H., H. Funahashi, L. R. Abeydeera, S. J. Moon, R. S. Prather, and B. N. Day. 1996. Effects of
463 oviductal fluid on sperm penetration and cortical granule exocytosis during fertilization of pig
464 oocytes in vitro. *Reproduction* 107:79–86.
- 465 Kirichok, Y., B. Navarro, and D. E. Clapham. 2006. Whole-cell patch-clamp measurements of
466 spermatozoa reveal an alkaline-activated Ca²⁺ channel. *Nature* 439:737–740.
- 467 Kirkman-Brown, J. C., and D. J. Smith. 2011. Sperm motility: is viscosity fundamental to progress?
468 *Molecular Human Reproduction* 17:539–544.
- 469 Lenth, R. V. 2016. Least-squares means: The R package “lsmeans.” *Journal of Statistical Software* 69:1–
470 33.
- 471 Lindemann, C. B., and J. S. Goltz. 1988. Calcium regulation of flagellar curvature and swimming pattern
472 in triton X-100–extracted rat sperm. *Cell Motility* 10:420–431.
- 473 Lishko, P. V., I. L. Botchkina, A. Fedorenko, and Y. Kirichok. 2010. Acid extrusion from human
474 spermatozoa is mediated by flagellar voltage-gated proton channel. *Cell* 140:327–337.
- 475 López-Albors, O., P. J. Llamas-López, J. Á. Ortuño, R. Latorre, and F. A. García-Vázquez. 2021. In vivo
476 measurement of pH and CO₂ levels in the uterus of sows through the estrous cycle and after
477 insemination. *Sci Rep* 11:3194.
- 478 Lüpold, S., J. B. Reil, M. K. Manier, V. Zeender, J. M. Belote, and S. Pitnick. 2020. How female × male
479 and male × male interactions influence competitive fertilization in *Drosophila melanogaster*.
480 *Evolution Letters* 4:416–429.

- 481 Manier, M. K., J. M. Belote, K. S. Berben, D. Novikov, W. T. Stuart, and S. Pitnick. 2010. Resolving
482 mechanisms of competitive fertilization success in *Drosophila melanogaster*. *Science* 328:354–
483 357.
- 484 Marquez, B., and S. S. Suarez. 2007. Bovine sperm hyperactivation is promoted by alkaline-stimulated
485 Ca²⁺ influx. *Biology of Reproduction* 76:660–665.
- 486 Martin-Coello, J., H. Dopazo, L. Arbiza, J. Ausió, E. R. S. Roldan, and M. Gomendio. 2009. Sexual
487 selection drives weak positive selection in protamine genes and high promoter divergence,
488 enhancing sperm competitiveness. *Proceedings of the Royal Society B: Biological Sciences*
489 276:2427–2436.
- 490 Miki, K., and D. E. Clapham. 2013. Rheotaxis guides mammalian sperm. *Current Biology* 23:443–452.
- 491 Miller, D. J. 2018. Review: The epic journey of sperm through the female reproductive tract. *Animal*
492 12:s110–s120.
- 493 Ng, K. Y. B., R. Mingels, H. Morgan, N. Macklon, and Y. Cheong. 2018. In vivo oxygen, temperature
494 and pH dynamics in the female reproductive tract and their importance in human conception: a
495 systematic review. *Human Reproduction Update* 24:15–34.
- 496 Orr, T. J., M. Burns, K. Hawkes, K. E. Holekamp, K. A. Hook, C. C. Josefson, A. A. Kimmitt, A. K.
497 Lewis, S. E. Lipshutz, K. S. Lynch, L. K. Sirot, D. J. Stadtmauer, N. L. Staub, M. F. Wolfner, and
498 V. Hayssen. 2020. It takes two to tango: including a female perspective in reproductive biology.
499 *Integrative and Comparative Biology* 60:796–813.
- 500 Overstreet, J. W., and G. W. Cooper. 1979. Effect of ovulation and sperm motility on the migration of
501 rabbit spermatozoa to the site of fertilization. *Reproduction* 55:53–59.
- 502 Parker, G. A. 1970. Sperm competition and its evolutionary consequences in the insects. *Biological*
503 *Reviews* 45:525–567.
- 504 Patczai, B., T. Mintál, L. G. Nót, N. Wiegand, and D. Lőrinczy. 2017. Effects of deep-freezing and
505 storage time on human femoral cartilage. *Journal of Thermal Analysis and Calorimetry*
506 127:1177–1180.

- 507 Petrunkina, A. M., J. Friedrich, W. Drommer, G. Bicker, D. Waberski, and E. Töpfer-Petersen. 2001.
508 Kinetic characterization of the changes in protein tyrosine phosphorylation of membranes,
509 cytosolic Ca²⁺ concentration and viability in boar sperm populations selected by binding to
510 oviductal epithelial cells. *Reproduction* 122:469–480.
- 511 Pizzari, T., and T. R. Birkhead. 2000. Female feral fowl eject sperm of subdominant males. *Nature*
512 405:787–789.
- 513 R Core Team. 2016. *R: A Language and Environment for Statistical Computing*. Vienna, Austria.
514 R Foundation for Statistical Computing. Retrieved from <https://www.R-project.org/>
- 515 Ramm, S. A., L. McDonald, J. L. Hurst, R. J. Beynon, and P. Stockley. 2009. Comparative proteomics
516 reveals evidence for evolutionary diversification of rodent seminal fluid and its functional
517 significance in sperm competition. *Molecular Biology and Evolution* 26:189–198.
- 518 Rodríguez-Martínez, H., F. Saravia, M. Wallgren, P. Tienthai, A. Johannisson, J. M. Vázquez, E.
519 Martínez, J. Roca, L. Sanz, and J. J. Calvete. 2005. Boar spermatozoa in the oviduct.
520 *Theriogenology* 63:514–535.
- 521 Rowe, M., L. Veerus, P. Trosvik, A. Buckling, and T. Pizzari. 2020. The reproductive microbiome: An
522 emerging driver of sexual selection, sexual conflict, mating systems, and reproductive isolation.
523 *Trends in Ecology & Evolution* 35:220–234.
- 524 Saito, K., Y. Kinoshita, H. Kanno, and A. Iwasaki. 1996. The role of potassium ion and extracellular
525 alkalization in reinitiation of human spermatozoa preserved in electrolyte-free solution at 4°C.
526 *Fertility and Sterility* 65:1214–1218.
- 527 Simmons, L. W., and J. L. Fitzpatrick. 2012. Sperm wars and the evolution of male fertility. *Reproduction*
528 144:519–534.
- 529 Simmons, L. W., and N. Wedell. 2020. Fifty years of sperm competition: the structure of a scientific
530 revolution. *Philosophical Transactions of the Royal Society B: Biological Sciences*
531 375:20200060.

- 532 Simons, J. E., and S. D. Olson. 2018. Sperm motility: models for dynamic behavior in complex
533 environments. In M. Stolarska and N. Tarfulea (Eds.), *Cell Movement* (pp. 169–209).
534 Switzerland: Birkhäuser.
- 535 Smith, D. J., E. A. Gaffney, H. Gadêlha, N. Kapur, and J. C. Kirkman-Brown. 2009. Bend propagation in
536 the flagella of migrating human sperm, and its modulation by viscosity. *Cell Motility and the*
537 *Cytoskeleton* 66:220–236.
- 538 Stival, C., L. del C. Puga Molina, B. Paudel, M. G. Buffone, P. E. Visconti, and D. Krapf. 2016. Sperm
539 capacitation and acrosome reaction in mammalian sperm. In M. G. Buffone (Ed.), *Sperm*
540 *Acrosome Biogenesis and Function During Fertilization* (pp. 93–106). Switzerland: Springer.
- 541 Suarez, S. S. 2008. Control of hyperactivation in sperm. *Human Reproduction Update* 14:647–657.
- 542 Suarez, S. S. 2016. Mammalian sperm interactions with the female reproductive tract. *Cell and Tissue*
543 *Research* 363:185–194.
- 544 Suarez, S. S., K. Brockman, and R. Lefebvre. 1997. Distribution of mucus and sperm in bovine oviducts
545 after artificial insemination: The physical environment of the oviductal sperm reservoir. *Biology*
546 *of Reproduction* 56:447–453.
- 547 Suarez, S. S., and X. Dai. 1995. Intracellular calcium reaches different levels of elevation in
548 hyperactivated and acrosome-reacted hamster sperm. *Molecular Reproduction and Development*
549 42:325–333.
- 550 Suarez, S. S., and H. C. Ho. 2003. Hyperactivation of mammalian sperm. *Cellular and Molecular Biology*
551 49:351–356.
- 552 Suárez, S. S., and R. A. Osman. 1987. Initiation of hyperactivated flagellar bending in mouse sperm
553 within the female reproductive tract. *Biology of Reproduction* 36:1191–1198.
- 554 Suarez, S. S., S. M. Varosi, and D. Xiaobing. 1993. Intracellular calcium increases with hyperactivation
555 in intact, moving hamster sperm and oscillates with the flagellar beat cycle. *Proceedings of the*
556 *National Academy of Sciences* 90:4660–4664.

- 557 Thornhill, R. 1983. Cryptic female choice and its implications in the scorpionfly *Harpobittacus nigriceps*.
558 The American Naturalist 122:765–788.
- 559 Troisi, A., and M. Carosi. 1998. Female orgasm rate increases with male dominance in Japanese
560 macaques. Animal Behaviour 56:1261–1266.
- 561 Tung, C., L. Hu, A. G. Fiore, F. Ardon, D. G. Hickman, R. O. Gilbert, S. S. Suarez, and M. Wu. 2015.
562 Microgrooves and fluid flows provide preferential passageways for sperm over pathogen
563 *Tritrichomonas foetus*. Proceedings of the National Academy of Sciences 112:5431–5436.
- 564 Tung, C.-K., and S. S. Suarez. 2021. Co-adaptation of physical attributes of the mammalian female
565 reproductive tract and sperm to facilitate fertilization. Cells 10:1297.
- 566 Turner, L. M., A. R. Young, H. Römler, T. Schöneberg, S. M. Phelps, and H. E. Hoekstra. 2010.
567 Monogamy evolves through multiple mechanisms: evidence from V1aR in deer mice. Molecular
568 Biology and Evolution 27:1269–1278.
- 569 Vahed, K., and D. J. Parker. 2012. The evolution of large testes: sperm competition or male mating rate?
570 Ethology 118:107–117.
- 571 Wickham, H. 2016. *ggplot2: Elegant Graphics for Data Analysis*. Springer.
- 572 Yanagimachi, R. 1982. Requirement of extracellular calcium ions for various stages of fertilization and
573 fertilization-related phenomena in the hamster. Gamete Research 5:323–344.
- 574 Yániz, J. L., F. Lopez-Gatius, P. Santolaria, and K. J. Mullins. 2000. Study of the functional anatomy of
575 bovine oviductal mucosa. The Anatomical Record 260:268–278.
- 576 Yeung, C.-H., S. Breton, I. Setiawan, Y. Xu, F. Lang, and T. G. Cooper. 2004. Increased luminal pH in
577 the epididymis of infertile c-ros knockout mice and the expression of sodium–hydrogen
578 exchangers and vacuolar proton pump H⁺-ATPase. Molecular Reproduction and Development
579 68:159–168.
- 580 Yuana, Y., A. N. Böing, A. E. Grootemaat, E. van der Pol, C. M. Hau, P. Cizmar, E. Buhr, A. Sturk, and
581 R. Nieuwland. 2015. Handling and storage of human body fluids for analysis of extracellular
582 vesicles. Journal of Extracellular Vesicles 4:29260.

583 Zhou, J., L. Chen, J. Li, H. Li, Z. Hong, M. Xie, S. Chen, and B. Yao. 2015. The semen pH affects sperm
584 motility and capacitation. PLOS ONE 10:e0132974.
585

586 **Tables and Figures**

587

588 **Table 1.** Mean (\pm SE) viscosity (Pa*s) of female reproductive tract fluids extracted from

589 *Peromyscus* mice that naturally vary by mating system

590

Mating system	<i>Peromyscus</i> species	Viscosity (Pa * s)		Linear model results from within species comparisons
		Uterus	Oviduct	
Polyandrous	<i>P. maniculatus</i>	0.04 \pm 0.02 (337)	0.02 \pm 0.01 (424)	$F_{1,759} = 175.9, p < 0.001$
	<i>P. leucopus</i>	8.8 \pm 6.6 (115)	0.006 \pm 0.002 (17)	$F_{1,130} = 4.528, p = 0.035$
	<i>P. gossypinus</i>	0.002 \pm 2.2e-04 (123)	0.001 \pm 5.8e-05 (130)	$F_{1,251} = 0.28, p = 0.597$
	Mean \pm SE	1.79 \pm 1.32	0.01 \pm 0.01	
Monogamous	<i>P. californicus</i>	0.29 \pm 0.14 (258)	0.04 \pm 0.03 (72)	$F_{1,328} = 16.76, p < 0.001$
	<i>P. eremicus</i>	0.004 \pm 8.1e-04 (35)	0.25 \pm 0.25 (251)	$F_{1,284} = 28.34, p < 0.001$
	<i>P. polionotus</i>	0.35 \pm 0.22 (389)	0.86 \pm 0.49 (863)	$F_{1,1250} = 111.3, p < 0.001$
	Mean \pm SE	0.31 \pm 0.14	0.68 \pm 0.36	

591

592

593 The number of tracked particles for each sample is indicated within parentheses. Linear models included

594 log-transformed viscosity values as the response variable and the region of the reproductive tract as the

595

596

597

598

599

600

601

602

603

604

605

606

607

608

609

610

611

612

613

Table 2. Mean (\pm SE) pH and calcium concentration of female reproductive fluids collected from two sister species of *Peromyscus* mice that vary in their mating system

Mating system	Species	pH		Calcium concentration ($\mu\text{m}/\mu\text{L}$)	
		Uterus	Oviduct	Uterus	Oviduct
Polyandrous	<i>P. maniculatus</i>	8.00 \pm 0.00	7.44 \pm 0.03	5.73 \pm 0.97	2.84 \pm 0.42
Monogamous	<i>P. polionotus</i>	7.76 \pm 0.06	7.28 \pm 0.03	4.11 \pm 0.40	3.22 \pm 0.53

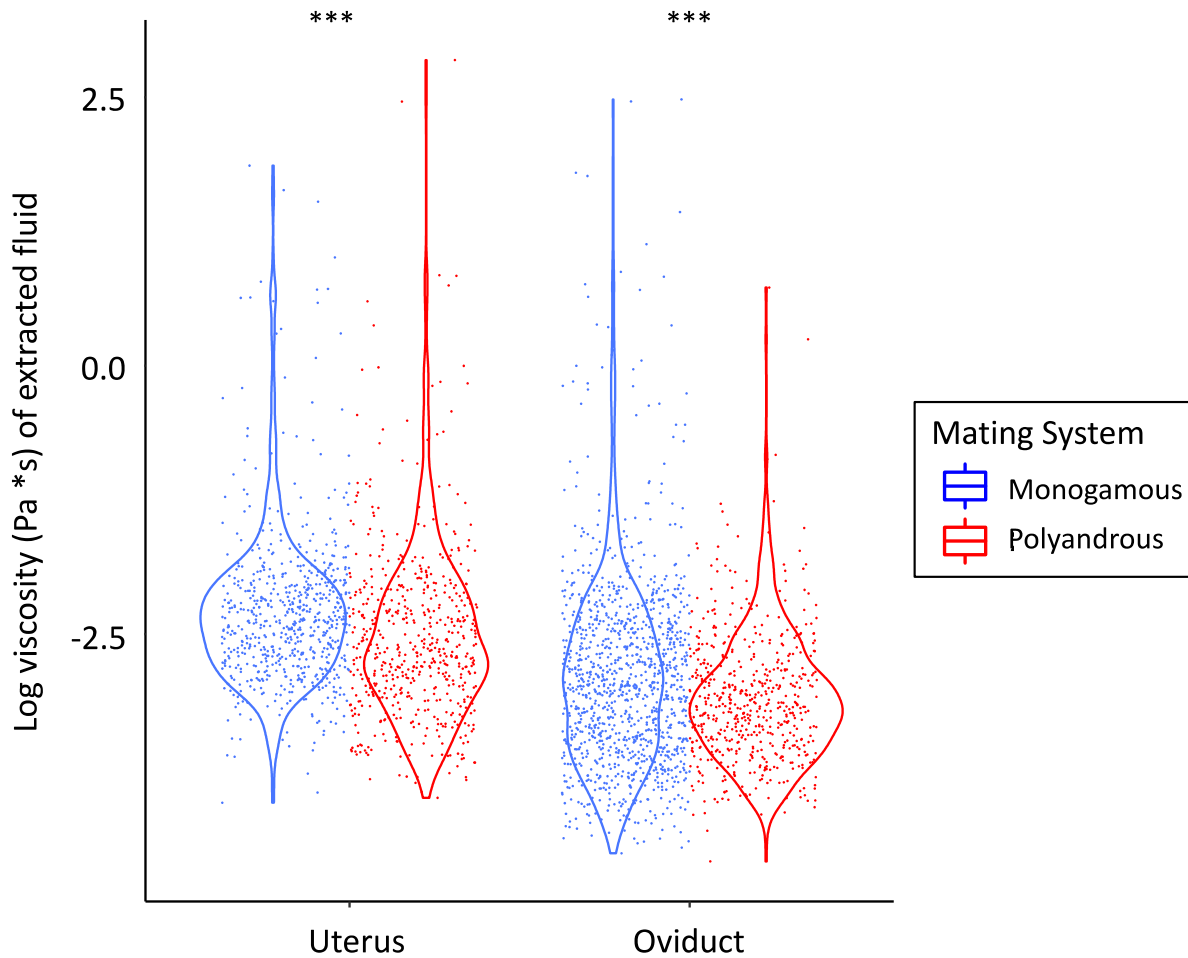


Figure 1. Violin plots of the log-transformed viscosity measurements obtained from fluids collected from two regions of the female reproductive tract within *Peromyscus* mice species with naturally varying mating systems. Blue dots represent particle tracking data obtained from three monogamous species (*P. californicus*, *P. eremicus*, and *P. polionotus*), red dots represent particle tracking data obtained from three polyandrous species (*P. maniculatus*, *P. leucopus*, and *P. gossypinus*). Asterisks denote differences within each reproductive region between the mating systems (***) $P < 0.001$).

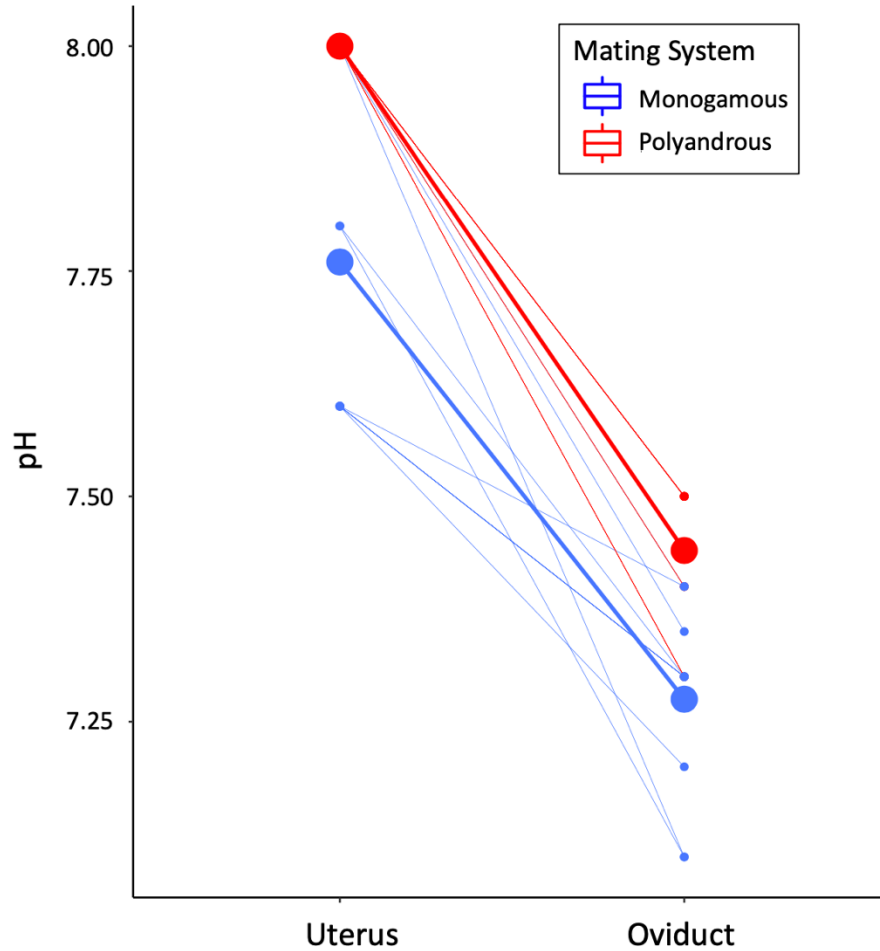


Figure 2. pH measurements obtained from fluids collected from the female reproductive tracts of *Peromyscus* mice species with naturally varying mating systems. In both the uterus and the oviduct, reproductive fluids have a significantly greater pH in the polyandrous *P. maniculatus* (red dots) than its monogamous sister species, *P. polionotus* (blue dots). Small dots denote values measured for individual females; large dots represent the mean values for each species.

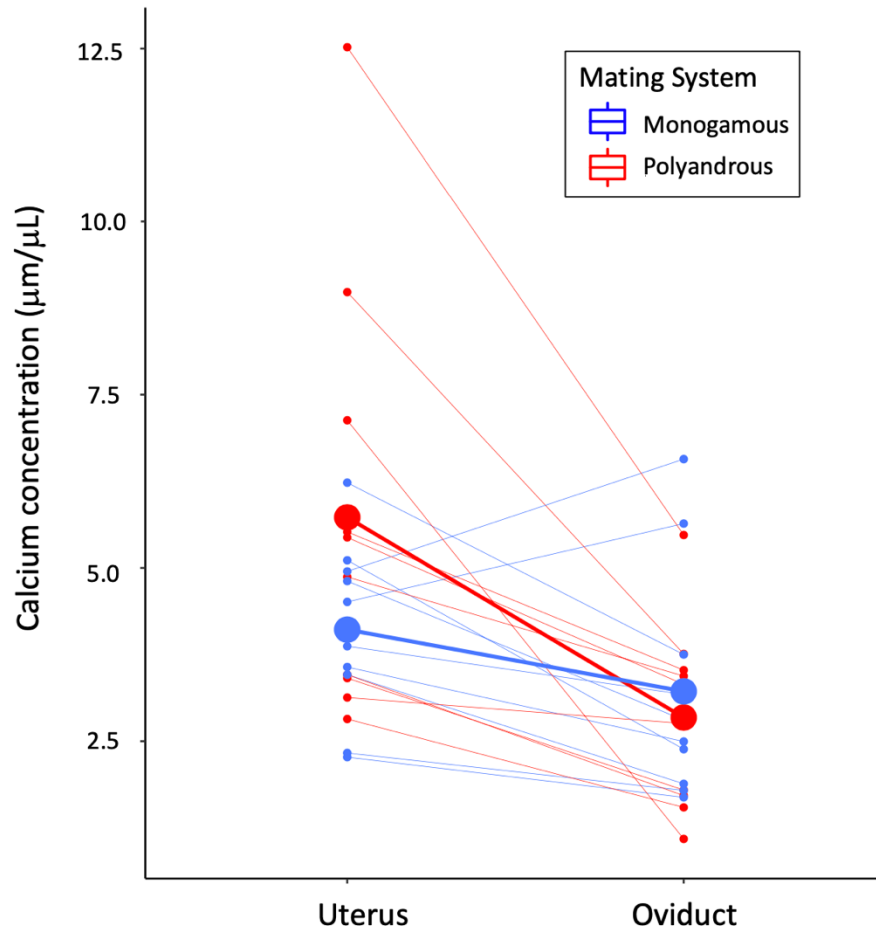


Figure 3. Calcium concentration measurements obtained from fluids collected from the female reproductive tracts of *Peromyscus* mice species with naturally varying mating systems. The calcemic content of reproductive fluids collected from the uterus and oviduct did not significantly differ between the polyandrous *P. maniculatus* (red dots) and its monogamous sister species, *P. polionotus* (blue dots). The calcium concentration between these regions significantly differed only for *P. maniculatus*. Small dots denote values measured for individual females; large dots represent the mean values for each species.

